Research Square

Preprints are preliminary reports that have not undergone peer review.
They should not be considered conclusive, used to inform clinical practice,
or referenced by the media as validated information.

Enabling p-Type Doping in Ionic Wide-Gap Semiconductors through Geometric Frustration

Chen Qiu
Eastern Institute of Technology
Xiao-Lan Yan
Eastern Institute of Technology
Su-Huai Wei
suhuaiwei@eitech.edu.cn

Eastern Institute of Technology

Article

Keywords:

Posted Date: November 26th, 2026

DOI: https://doi.org/10.21203/rs.3.rs-11057866/v1

License: This work is licensed under a Creative Commons Attribution 4.0 International License.
Read Full License

Additional Declarations: No competing interests reported.

Enabling p-Type Doping in Ionic Wide-Gap Semiconductors through Geometric Frustration

Chen Qiu[1,#], Xiao-Lan Yan[1,#] , Su-Huai Wei[1,*]
[1] School of Physics, Eastern Institute of Technology, Ningbo 315200, China

The p-type carrier density depends exponentially on the separation between the equilibrium Fermi level and the valence-band maximum (VBM). In the past, the prevailing materials-design strategy to increase the carrier density is raising the VBM through band-edge engineering. Here we demonstrate a complementary route that shifts the Fermi level toward the VBM through lattice-topology control. By comparing the wurtzite and rocksalt polymorphs of ZnO, we demonstrate that the close-packed rocksalt topology raises the formation energies of the p-type killer defects Li_i and Na_i by 1.39 and 2.20 eV, respectively, while leaving the desired p-type substitutional acceptors Li_{Zn} and Na_{Zn} nearly unchanged. This site selectivity removes dopant self-compensation as the active Fermi-level pinning cause, thus significantly improves the p-type dopability. Based on these understandings, we combine geometric suppression of interstitial donors with band edge engineering to achieve p-type doping in wide-band-gap rocksalt SrX (X = O, S, Se, Te). We show that from SrO to SrTe, the rising anion-derived VBM weakens native-donor compensation, and self-consistent finite-temperature defect-thermodynamic calculations predict room-temperature hole concentrations of approximately 5×10^{17} cm^{-3} in quenched Na- and K-doped SrTe. These results establish a dual design principle for p-type wide-gap semiconductors: combine favorable band-edge energetics with lattice topologies that preserve desired acceptors while suppressing compensating donors.

# These authors contributed equally to this work.
* Electronic mail: suhuaiwei@eitech.edu.cn

Introduction—In the nondegenerate regime, the hole concentration is given by $p = N_v exp[-(E_F - E_{VBM})/(k_B T)]$[1], where N_v is the effective valence band density of state, E_F is the Fermi level, and E_{VBM} is the valence band maximum (VBM) energy. At a given temperature, the free-hole concentration is exponentially dependent on the separation $\Delta\varepsilon_F = E_F - E_{VBM}$. Therefore, to increase the hole concentration, one should reduce the value of $\Delta\varepsilon_F$ by either raising the VBM energy or lowering the Fermi level toward the VBM. However, the reduction of the $\Delta\varepsilon_F$ is limited as explained by the doping-limit rule: as E_F approaches the VBM, the formation energies of positively charged compensating defects decrease until they can form spontaneously, thus pinning the Fermi level[2-5]. Therefore, to overcome this doping limit, in the past, materials-design strategies inspired by this framework have predominantly focused on band-edge engineering to push up the VBM energy[6-13].

Here we identify a complementary route to lower the pinning Fermi level by increasing the formation-energy of a compensating donor through lattice-topology control. This mechanism becomes decisive when extrinsic dopant can occupy crystallographic sites with opposite electrical activities [14-16]. In a divalent compound, for example, an alkali atom on the cation site is nominally an acceptor, whereas the same atom on an interstitial site is nominally a donor. The net doping response is, therefore, governed by the relative formation energies of these two configurations. A host lattice that selectively penalizes the interstitial donor without comparably penalizing the substitutional acceptor can shift the Fermi-level pinning position imposed by dopant self-compensation toward the VBM[17-23].

Band-edge alignment and local lattice geometry enter the same defect thermodynamics through physically distinct contributions. Band-edge alignment changes the electronic energy of charged defects relative to a common reference[24-26], while local geometry changes the structural contribution to their formation energies and the relative stability of competing dopant configurations. Tetrahedrally coordinated semiconductors often contain open interstitial cavities in which substitutional acceptors and interstitial donors can coexist. By contrast, the occupied octahedral network of a rocksalt lattice leaves only residual tetrahedral voids, which can impose a large strain penalty on interstitial incorporation[27,28]. These real-space features of crystal structures raise a central question: can lattice topology be formulated as a transferable criterion for selectively increasing the formation energy of compensating interstitial donors and, together with favorable band-edge alignment, suppress both dopant self-compensation and native-defect compensation?

Here, we first isolate how lattice topology shifts the dopant-self-compensation pinning level toward the VBM and then combine this structural mechanism with band-edge control. A controlled comparison of the wurtzite and rocksalt polymorphs of ZnO shows that the rocksalt topology selectively destabilizes alkali interstitial donors without comparably penalizing cation-site acceptors, thereby shifting the Fermi-level-limiting mechanism from dopant self-compensation to native-donor compensation. Because the

two polymorphs have similar native-defect pinning levels, however, topology-induced site selectivity alone cannot overcome native compensation. We therefore test the combined criterion in rocksalt SrX (X = O, S, Se, and Te), where the constrained residual interstitial sites penalize interstitial incorporation of alkali dopants, while the progressively rising anion-p-derived VBM from SrO to SrTe weakens native-donor compensation and stabilizes substitutional acceptors. Self-consistent finite-temperature defect thermodynamic calculations predict room-temperature hole densities of ~5×10^{17} cm^{-3} for Na- and K-doped SrTe grown under anion-rich conditions and subsequently quenched. Together, these results establish a dual design principle for p-type wide-gap semiconductors: combine a lattice that geometrically frustrates interstitial donors with a sufficiently high VBM to suppress native-donor compensation.

Method—Density-functional theory (DFT) calculations were performed using the Vienna Ab Initio Simulation Package (VASP)[29]. Exchange-correlation interactions were described using the generalized gradient approximation (GGA) in the Perdew-Burke-Ernzerhof (PBE) form[30,31]. To achieve an improved description of electronic structures and defect energetics, the screened hybrid functional of Heyd-Scuseria-Ernzerhof (HSE06)[32,33] was further employed. See Supplemental Material for more methodological information[25,34-37].

Geometry-controlled site selectivity—To identify the geometric origin of dopant site selectivity, we first use ZnO as a controlled model system and compare two coordination topologies with the same chemical composition, tetrahedrally coordinated wurtzite ZnO and octahedrally coordinated rocksalt ZnO. In the wurtzite lattice, the relevant interstitial site is a trigonal-prismatic cavity bounded by three O and three Zn atoms, see Figure 1a and 1b. In contrast, the rocksalt lattice has all octahedral sites occupied by the two interpenetrating sublattices, leaving only tetrahedral residual voids (Figure 1d and 1e). Within an idealized hard-sphere construction, the centered free radius of the wurtzite cavity is at least 55% larger than that of the rocksalt tetrahedral void for the same cation and anion radius (Supplemental Material for derivation). The structural transformation therefore changes not only the coordination number but also the configuration space available to an interstitial impurity.

We then examine whether this geometric constraint is reflected in the defect thermodynamics of alkali-metal dopants. As shown in Figure 1c and 1f, substitutional acceptors A_{Zn} (A=Li, Na) have comparable formation energies in wurtzite and rocksalt ZnO under O-rich conditions. The slightly lower A_{Zn} formation energies in rocksalt ZnO indicate that changing the coordination topology favors acceptor incorporation on the Zn site, but this is a secondary effect. The dominant change instead occurs for donor-like interstitials. Relative to wurtzite ZnO, the formation energy of Li_i increases by about 1.39 eV in rocksalt ZnO, while that of Na_i increases by more than 2.20 eV. The rocksalt lattice therefore acts as a site-selective energy filter in which incorporation on the Zn substitutional site remains

accessible, whereas incorporation at the interstitial site is strongly penalized.

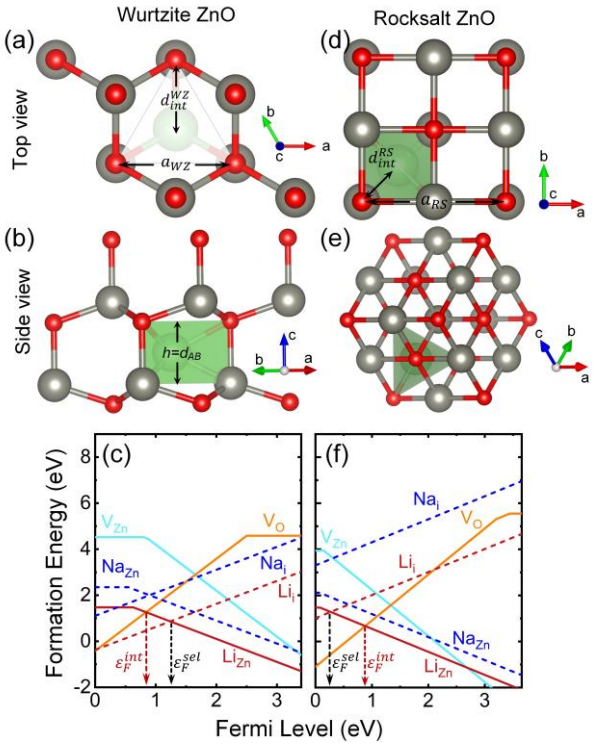

Figure 1. Lattice topology switches the compensation mechanism of alkali-metal dopants in ZnO. a, b) Top and side views of the representative interstitial void in wurtzite ZnO. The interstitial site forms a trigonal-prismatic cavity bounded by three O and three Zn atoms, with center-to-neighbor distance d_{int}^{WZ}. d, e) Corresponding tetrahedral interstitial void in rocksalt ZnO, with center-to-neighbor distance d_{int}^{RS}. The hard-sphere geometry shows that the tetrahedrally coordinated wurtzite lattice provides a larger interstitial void than the octahedrally coordinated rocksalt lattice. c, f) Calculated formation energies of group-IA impurities Li and Na in wurtzite and rocksalt ZnO under O-rich conditions. The dashed vertical arrows mark the pinning positions associated with dopant self-compensation (ε_F^{sel}) and intrinsic-defect compensation (ε_F^{int}).

This selective destabilization changes the compensation mechanism that limits the Fermi level. In wurtzite ZnO, Li_{Zn} acceptors and Li_i donors coexist with comparable formation energies near the pinning Fermi level, i.e., the Fermi level is pinned by substitutional-interstitial self-compensation. The corresponding pinning positions are approximately 1.24 eV above the VBM, indicating very low hole carrier density. In rocksalt ZnO, this self-compensation channel is strongly weakened: the Li-induced substitutional-interstitial pinning collapses to about 0.27 eV above the VBM. Once dopant self-compensation ceases to be the active limiting cause, however, the achievable Fermi-level position is no longer determined by Li_{Zn}-Li_i competition but by native donor compensation. Because the native-defect pinning levels in wurtzite and rocksalt ZnO remain similar (about 0.8 eV), the suppression of interstitial dopants alone does not make rocksalt ZnO an optimal p-type wide-gap semiconductor. Rather, ZnO isolates the real-space part of the dopability problem that lattice topology can suppress dopant self-

compensation as the active Fermi-level limit, but a favorable band-edge position is still required to suppress native compensation. This result motivates a dual design strategy in which geometrically frustrated interstitial sites are combined with a high VBM in materials sharing the same rocksalt topology.

Having established this principle in a controlled ZnO model, we next ask whether it can be realized in stable wide-gap semiconductors. Tetrahedrally coordinated II-VI compounds such as ZnO are relatively covalent and contain open interstitial cavities, whereas more ionic AB compounds tend to favor higher coordination structures because their bonding is less directional and their Coulomb interaction is stronger[38,39]. This consideration naturally points to alkaline-earth chalcogenides[40-43]. In particular, IIA-VI compounds contain large, electropositive alkaline-earth cations and crystallize in rocksalt structures over a broad chemical range, making them suitable platforms for testing whether rocksalt geometry can promote p-type dopability.

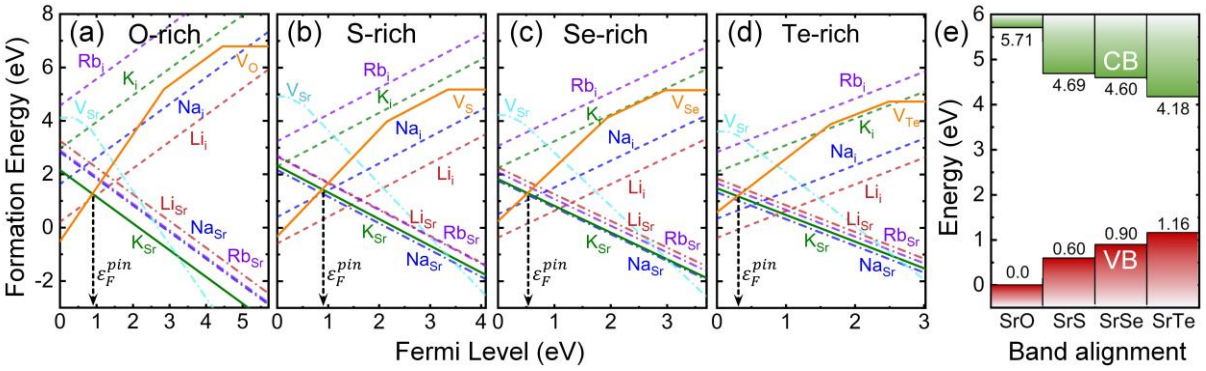

Figure 2. Defect thermodynamics and band-edge evolution in rocksalt SrX (X = O, S, Se, Te). a-d) Calculated formation energies of native vacancies and group-IA-related defects in rocksalt a) SrO, b) SrS, c) SrSe and d) SrTe under anion-rich conditions as a function of the Fermi level. e) Calculated band alignment of SrO, SrS, SrSe, and SrTe. The upward shift of the VBM from SrO to SrTe stabilizes acceptor defects and destabilizes donor-like compensating defects, providing the electronic origin of the improved p-type dopability.

We therefore examine rocksalt SrX (X = O, S, Se, Te) as representative ionic wide-gap semiconductors. Figure 2 shows the calculated formation energies of native vacancies and group-IA impurities under anion-rich conditions. A common feature across the SrX series is the large energetic separation between substitutional acceptors and interstitial donors. For alkali impurities, the formation energies of interstitial configurations A_i (A = Li, Na, K, Rb) increase strongly with impurity size, reflecting the structural penalty for placing large monovalent dopants into the residual tetrahedral voids of the rocksalt lattice. In contrast, substitutional acceptors A_{Sr} are most favorable when the dopant radius is well matched to the Sr site. Among the alkali-metal dopants, Na and K provide the most favorable balance between low substitutional-acceptor formation energies and suppressed interstitial-donor compensation, with K showing particularly robust site selectivity across the SrX series.

The structural origin of this energetic separation is revealed by the relaxed local geometries in

Figure 3. We quantify the impurity-induced distortion by the average change in the neighboring host cation-anion bond lengths relative to the pristine lattice. For every group-IA impurity considered, interstitial incorporation produces substantially larger bond-length reduction in neighboring atoms in rocksalt SrX than in wurtzite ZnO, and the distortion increases systematically from Li to Rb with increasing impurity radius. By contrast, the more open interstitial cavities in wurtzite ZnO accommodate alkali impurities with much smaller changes to the surrounding Zn-O bonds. These results directly connect the geometrically constrained tetrahedral voids of the rocksalt lattice to the enhanced structural penalty and high formation energies of interstitial donors, thereby preserving strong substitutional-interstitial site selectivity across the SrX series.

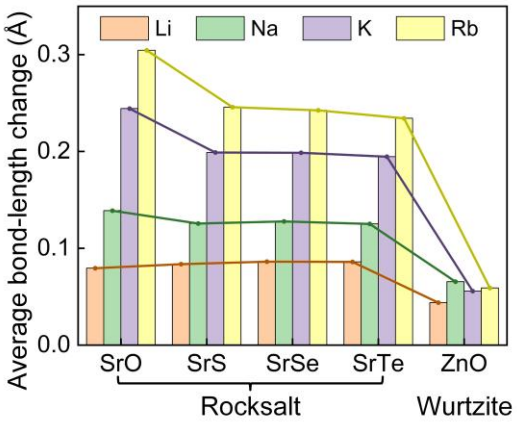

Figure 3. Local bond length reduction induced by interstitial group-IA impurities. Average changes in the neighboring host cation-anion bond lengths after the incorporation of interstitial Li, Na, K, and Rb in rocksalt SrX (X = O, S, Se, Te) and wurtzite ZnO. Interstitial incorporation produces substantially larger bond-length distortions in the rocksalt SrX compounds than in wurtzite ZnO. Within the rocksalt series, the distortion increases systematically with the size of the alkali impurity, demonstrating the growing structural penalty for accommodating large dopants in the geometrically constrained tetrahedral interstitial voids. For Wurtzite ZnO, the balance between strain and Coulomb interaction makes the changes small.

Once donor-like interstitials are geometrically suppressed, the dominant compensation mechanism shifts to native donor defects, especially anion vacancies V_X. The trend of V_X across the SrX series reflects the competition between bond breaking and band-edge energetics. From SrO to SrTe, the Sr-X bond becomes longer and weaker, which tends to lower the formation energy of the neutral V_X. However, the compensating charge-state relevant to p-type doping is donor-like and positively charged. As shown by the band alignment in Figure 2e, the anion *p*-orbital derived VBM moves upward systematically from SrO to SrTe (projected band structure in Figure S5). This upward VBM shift raises the formation energy of positively charged donor defects near the VBM, including (V_X), while simultaneously stabilizing negatively charged substitutional acceptors (A_{Sr}). As a result, the formation

energies of group-IA substitutional acceptors A_{Sr} decrease from SrO to SrTe, whereas the donor-like anion vacancies V_X become less effective at pinning the Fermi level.

This opposite evolution of acceptor and donor formation energies leads to a systematic improvement in p-type dopability across the SrX series. The calculated Fermi-level pinning position moves progressively toward the VBM, from approximately 0.89 eV in SrO and 0.88 eV in SrS to 0.52 eV in SrSe and 0.30 eV in SrTe. The improvement is therefore not controlled by a single factor. Rocksalt geometry provides a real-space site-selectivity descriptor by penalizing interstitial donor incorporation, whereas the upward shift of the VBM provides an electronic-structure descriptor by stabilizing acceptors and destabilizing positively charged native donors. These two descriptors together define a design principle for p-type wide-gap semiconductors: an optimal host should combine geometrically frustrated interstitial sites with a sufficiently high valence-band edge.

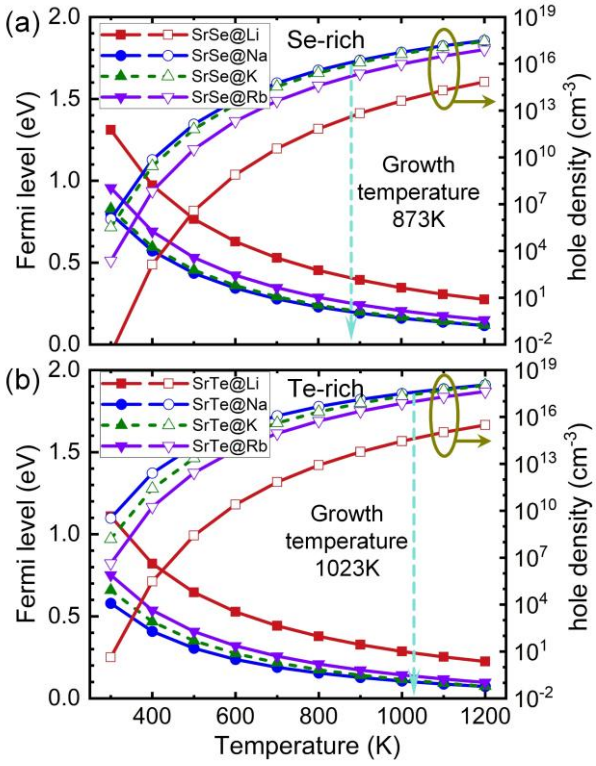

Figure 4. Post-quench room-temperature Fermi-level positions and hole concentrations as functions of growth temperature for group-IA-doped a) SrSe and b) SrTe under anion-rich conditions. The total concentration of each atomic defect species is established at and frozen upon quenching, whereas defect charge states, free carriers, and the Fermi level are re-equilibrated at 300 K. Filled symbols denote the Fermi-level positions, and open symbols denote the corresponding hole concentrations. The dopants considered are Li, Na, K, and Rb on Sr sites, with compensating native and impurity-related defects included in the charge-neutrality condition. The vertical dashed arrows indicate representative growth temperatures, 873 K for SrSe and 1023 K for SrTe.

The preceding results indicate that rocksalt SrSe and SrTe combine the two conditions required for

p-type dopability: geometrically suppressed interstitial donors and relatively shallow Fermi-level pinning by native donor defects. We therefore examine whether these thermodynamic advantages can be converted into finite carrier concentrations through high-temperature quenching. In this non-equilibrium doping protocol, defect concentrations are established at the growth temperature and then frozen by rapid quenching, while the electronic carriers and defect charge states are allowed to re-equilibrate at the measurement temperature. Because higher growth temperatures increase the total concentration of incorporated acceptors, quenching can enhance the achievable hole density beyond the value expected from low-temperature equilibrium.

Figure 4 shows the calculated quasi-equilibrium Fermi levels and hole concentrations of group-IA-doped SrSe and SrTe under anion-rich conditions as a function of growth temperature. The trends are consistent with the defect thermodynamics in Figure 2. Li yields modest hole densities because its small-size leaves Li_i comparatively accessible, leading to strong self-compensation of Li_{Sr}. Rb exhibits the opposite limitation. Rb_i is strongly suppressed, but the larger substitutional formation energy restricts Rb_{Sr} incorporation. Na and K therefore achieve the most favorable balance between acceptor incorporation and suppression of compensating interstitials. As the growth temperature increases, the Fermi level moves closer to the VBM and the hole concentration increases systematically, showing that acceptor incorporation rather than compensating donor formation controls the quench-limited carrier density.

At representative growth temperatures based on previous synthesis reports, SrSe doped with Na or K reaches hole concentrations on the order of 10^{16} cm^{-3} at 873 K[44], whereas SrTe reaches hole concentrations approximately 5×10^{17} cm^{-3} at 1023 K[45,46]. These values demonstrate that the site-selective suppression of interstitial donors is not only a zero-temperature defect-formation-energy effect but also translates into finite-temperature p-type carrier generation. Together with their wide band gaps and anion-*p*-derived valence bands, rocksalt SrSe and SrTe therefore emerge as promising p-type wide-gap semiconductors with potential relevance to transparent electronics[47,48].

Conclusion—Our results establish dopant-site selectivity as a real-space component of p-type dopability, complementary to the band-edge criterion embodied in the electronic structure. Band-edge positions control native-defect compensation by determining the formation energies of charged compensating defects, whereas lattice topology controls whether an extrinsic dopant can access compensating configurations. The comparison between wurtzite and rocksalt ZnO isolates this real-space effect. Changing the coordination topology from wurtzite to rocksalt selectively raises the formation energies of Li and Na interstitial donors while keeping substitutional acceptors accessible. As a result, the limiting mechanism switches from substitutional-interstitial self-compensation in wurtzite ZnO to native-defect compensation in rocksalt ZnO. However, because the native-defect pinning levels

remain similar in the two ZnO structures, suppressing interstitial dopants alone is insufficient to produce an optimal p-type wide-gap semiconductor. This controlled comparison shows that lattice topology can remove dopant self-pinning, but favorable band-edge positions are still required to overcome native donor compensation. Rocksalt SrX compounds implement this dual design principle in stable ionic wide-gap semiconductors. Their geometrically constrained interstitial sites frustrate alkali donor incorporation, while the rising anion-*p* valence band from SrO to SrTe reduces native-donor compensation. The combination of these two effects makes Na- and K-doped SrTe the most favorable case, with quenched hole densities exceeding 5×10^{17} cm^{-3}. Geometric frustration of interstitial donors therefore provides a real-space component of p-type dopability, complementary to the reciprocal-space component embodied in band-edge engineering. This dual criterion framework suggests a design route for p-type wide-gap semiconductors: combine a high valence-band edge with a lattice geometry that preserves acceptors while penalizing compensating donor configurations.

Acknowledgements—This work was supported by the National Natural Science Foundation of China (No. 12504090, No. 12688201), and the National Key Research and Development Program of China (Grant No. 2024YFA1409800).

[1] S. M. Sze and K. K. Ng, *Physics of Semiconductor Devices* 2006).
[2] S. B. Zhang, S.-H. Wei, and A. Zunger, J. Appl. Phys. **83**, 3192 (1998).
[3] S. B. Zhang, S. Wei, and A. Zunger, Phys. Rev. Lett. **84**, 1232 (2000).
[4] C. G. Van de Walle and J. Neugebauer, Nature **423**, 626 (2003).
[5] C. G. Van de Walle, Phys. Rev. B **39**, 1871 (1989).
[6] H. Kawazoe, M. Yasukawa, H. Hyodo, M. Kurita, H. Yanagi, and H. Hosono, Nature **389**, 939 (1997).
[7] Y. Ogo, H. Hiramatsu, K. Nomura, H. Yanagi, T. Kamiya, M. Hirano, and H. Hosono, Appl. Phys. Lett. **93**, 032113 (2008).
[8] Y. Ogo, H. Hiramatsu, K. Nomura, H. Yanagi, T. Kamiya, M. Kimura, M. Hirano, and H. Hosono, phys. stat. sol. (a) **206**, 2187 (2009).
[9] Z. Wu, C. Li, X. Hu, K. Chen, X. Guo, Y. Li, and L. Lu, Nat. Mater. **24**, 1387 (2025).
[10] J. Willis and D. O. Scanlon, J. Mater. Chem. C **9**, 11995 (2021).
[11] A. Goyal, P. Gorai, S. Anand, E. S. Toberer, G. J. Snyder, and V. Stevanović, Chem. Mater. **32**, 4467 (2020).
[12] A. M. Ganose, D. O. Scanlon, A. Walsh, and R. L. Z. Hoye, Nat. Commun. **13**, 4715 (2022).
[13] J. Robertson and Z. Zhang, MRS Bull. **46**, 1037 (2021).
[14] C. H. Park, S. B. Zhang, and S.-H. Wei, Phys. Rev. B **66**, 073202 (2002).
[15] K. Matsuzaki, N. Tsunoda, Y. Kumagai, Y. Tang, K. Nomura, F. Oba, and H. Hosono, J. Am. Chem. Soc. **144**, 16572 (2022).
[16] K. Matsuzaki, C. W. Chang, T. Nagafuji, N. Tsunoda, Y. Kumagai, K. Nomura, F. Oba, and H. Hosono, J. Am. Chem. Soc. **146**, 24630 (2024).
[17] E.-C. Lee and K. J. Chang, Phys. Rev. B **70**, 115210 (2004).

[18] G. Miceli and A. Pasquarello, Phys. Rev. B **93**, 165207 (2016).
[19] F. Tuomisto, V. Prozheeva, I. Makkonen, T. H. Myers, M. Bockowski, and H. Teisseyre, Phys. Rev. Lett. **119**, 196404 (2017).
[20] Y. Kumagai, Phys. Rev. Appl. **19**, 034063 (2023).
[21] Y. Xue, Z. Zhuo, C. Lin, and D. Huang, Physical Chemistry Chemical Physics **27**, 9396 (2025).
[22] Y. Zhu and Z. Xiao, J. Phys. Chem. Lett. **16**, 11144 (2025).
[23] Y. Kumagai, N. Tsunoda, A. Takahashi, and F. Oba, Phys. Rev. Mater. **5**, 123803 (2021).
[24] S. Lany and A. Zunger, Phys. Rev. Lett. **98**, 045501 (2007).
[25] S.-H. Wei, Comput. Mater. Sci. **30**, 337 (2004).
[26] A. Janotti and C. G. Van de Walle, Rep. Prog. Phys. **72**, 126501 (2009).
[27] A. Goyal and V. Stevanović, Phys. Rev. Mater. **2**, 084603 (2018).
[28] J. L. Lyons, Phys. Rev. Mater. **9**, 124602 (2025).
[29] G. Kresse and J. Furthmüller, Phys. Rev. B **54**, 11169 (1996).
[30] P. E. Blöchl, Phys. Rev. B **50**, 17953 (1994).
[31] J. P. Perdew, K. Burke, and M. Ernzerhof, Phys. Rev. Lett. **77**, 3865 (1996).
[32] J. Heyd, G. E. Scuseria, and M. Ernzerhof, J. Chem. Phys. **118**, 8207 (2003).
[33] A. V. Krukau, O. A. Vydrov, A. F. Izmaylov, and G. E. Scuseria, J. Chem. Phys. **125**, 224106 (2006).
[34] J.-H. Yang, W.-J. Yin, J.-S. Park, J. Burst, W. K. Metzger, T. Gessert, T. Barnes, and S.-H. Wei, J. Appl. Phys. **118**, 025102 (2015).
[35] Y.-H. Li, A. Walsh, S. Chen, W.-J. Yin, J.-H. Yang, J. Li, J. L. F. D. Silva, X. G. Gong, and S.-H. Wei, Appl. Phys. Lett. **94**, 212109 (2009).
[36] H.-X. Deng, J.-W. Luo, and S.-H. Wei, Phys. Rev. B **91**, 075315 (2015).
[37] C. Freysoldt, J. Neugebauer, and C. G. Van de Walle, Phys. Rev. Lett. **102**, 016402 (2009).
[38] J. C. Phillips, Rev. Mod. Phys. **42**, 317 (1970).
[39] L. Pauling, J. Am. Chem. Soc. **51**, 1010 (1929).
[40] M. Zhong, W. Zeng, F.-S. Liu, D.-H. Fan, B. Tang, and Q.-J. Liu, Materials Today Physics **22**, 100583 (2022).
[41] V.-A. Ha, G. Yu, F. Ricci, D. Dahliah, M. J. van Setten, M. Giantomassi, G.-M. Rignanese, and G. Hautier, Phys. Rev. Mater. **3**, 034601 (2019).
[42] Y. Chen, L. Yang, G. Y. Gao, and S. W. Fan, Materials Science and Engineering: B **285**, 115953 (2022).
[43] Y. Chen, S. W. Fan, and P. Xu, Appl. Phys. Lett. **121**, 252102 (2022).
[44] Y. Nakanishi, T. Suzuki, H. Tatsuoka, H. Kuwabara, H. Fujiyasu, Y. Fukuda, and G. Shimaoka, Vacuum **41**, 1454 (1990).
[45] J. Hauck, F.-J. Börgermann, and D. Willmann, Inorg. Chim. Acta **140**, 119 (1987).
[46] R. C. Ropp, in *Encyclopedia of the Alkaline Earth Compounds*2013), pp. 105.
[47] J. Kim, J. Choi, and Y. Kang, Curr. Appl. Phys. **48**, 90 (2023).
[48] R. Woods-Robinson, M. Morales-Masis, G. Hautier, and A. Crovetto, PRX Energy **3**, 031001 (2024).

Supplementary Files

This is a list of supplementary files associated with this preprint. Click to download.

- SupplementalMaterial.docx